Kinetics and Equilibria of Nickel(II)−Schiff Base Adducts Formation

Ivo Cacelli,[a] Laura Carbonaro,*[a] and Piero La Pegna[a]

Keywords: Kinetics / Nickel / Schiff base / Adducts / Substituent effects

The interactions between Ni^{II} cations and bidentate Schiff base ligands, *N*-alkyl-5-X-salicylaldimine HL (X = H; R = Et, *n*Pr, *t*Bu; X = Cl, OMe, NO_2; R = *n*Pr), and bis(*N*-*n*-alkyl-5-X-salicylaldiminato)nickel(II) complexes [NiL_2] (X = H; R = Et, *n*Pr, *n*Bu; X = Cl, OMe, Me; R = *n*Pr) were investigated by UV/Vis spectrophotometry in acetonitrile. The kinetics for the formation of Ni^{II}/HL 1:1 adducts was studied by stopped-flow techniques, which showed that the process followed a two-consecutive mechanism. Experimental evidence and theoretical calculations indicated the formation of an unidentate intermediate in the first step, according to a dissociative interchange mechanism. Ring-closure occurs in the second step and its rate is slower for electron-withdrawing-substituted Schiff bases. Nickel(II) cations interact with [NiL_2] affording $[NiL]^+$ and $[Ni_2L_3]^+$ species; the associated equilibrium constants were found to be related to the electronic effects of the 5-X ligand substituents.

Introduction

Metal adducts of Schiff bases are an important class of compounds. Metal complexes [ML_2] of Schiff bases derived from salicylaldehyde can form adducts with different ions,[1,2] and even with DNA.[3] Examples of $MA_n{\cdot}mHL$ adducts (A = anion) between neutral HL Schiff base ligands and metal ions have also been reported.[4] The nature and the factors influencing the observed stoichiometries of individual adducts have been investigated mainly with regard to the steric hindrance of the imine group. In spite of the interest in these compounds, not much information is available on both the stability constants and the kinetics for the formation of these compounds. This is the first investigation of the mechanism for the formation of 1:1 Ni^{II}/HL adducts in acetonitrile, and of the equilibria between Ni^{II} cations and [NiL_2] complexes (HL = 5-X-salH-R) for various 5-X aromatic ring substituents and nitrogen-bound aliphatic chains R of the Schiff base ligand, see Scheme1.

The mechanism of solvent exchange and ligand substitution involving octahedral nickel(II) ions has been shown to be dissociative in character and generally to proceed by the fast formation of an outer-sphere complex followed by the loss of a solvent molecule in the rate-determining step,[5] see Equations (1a and b). Thus, the pseudo-first-order rate constant is generally expressed by Equation (2), where K_0 is the equilibrium constant for the formation of the outer-sphere complex, k_2 can be approximated to the rate constant for solvent exchange k_{ex}, and k_{-2} is the first-order rate constant for the reverse dissociation process.

$$Z{\cdots}Y + [NiS_6]^{2+} \overset{K_0}{\rightleftharpoons} [NiS_6{\cdot}Z{\cdots}Y]^{2+} \quad (1a)$$

$$[NiS_6{\cdot}Z{\cdots}Y]^{2+} \underset{k_{-2}}{\overset{k_2}{\rightleftharpoons}} [S_5Ni{-}Z{\cdots}Y]^{2+} + S \quad (1b)$$

$$[S_5Ni{-}Z{\cdots}Y]^{2+} \underset{k_{-3}}{\overset{k_3}{\rightleftharpoons}} [S_4Ni\begin{matrix}Z\\|\\Y\end{matrix}]^{2+} + S \quad (1c) \qquad (1)$$

$$k_{obs} = k_f[Ni^{2+}] + k_d = K_0k_2[Ni^{2+}] + k_{-2} \qquad (2)$$

This mechanism can be extended to bidentate ligands by introducing an additional, usually fast, ring-closure step, see Equation (1c). It can be anticipated that bidentate 5-X-salH-R ligands give rise to ring-closure inhibition in the coordination reaction to nickel(II) cations, as they can form hydrogen bonds between their chelating sites, and may exist[6,7] in zwitterionic forms $HL^{\pm}$ in polar solvents (see Scheme 1). Differing from most of the kinetics studies reported in the literature on solvent substitution reactions by bidentate ligands, the steps according to Equations (1b and c) can be studied kinetically, and the substituent effects on the ring-closure step can be examined.

The interactions between [NiL′] tetradentate complexes (Scheme 1) and alkaline, alkaline-earth or Ni^{II} cations were previously studied by our group.[8] Adducts of stoichiometry 1:1 and/or 1:2 form in acetonitrile, see **1** and **2** of Scheme 2. Metal ions are coordinated by means of the O···O bite offered by the [NiL′] complex.

Solid-state examples of adducts formed between metal ions and bidentate [NiL_2] complexes (Scheme 1) are re-

[a] Dipartimento di Chimica e Chimica Industriale, Università di Pisa,
Via Risorgimento 35, 56126 Pisa, Italy
Fax: (internat.) + 39-050/918260
E-mail: laucb@dcci.unipi.it

Supporting information for this article is available on the WWW under http://www.eurjic.com or from the author.

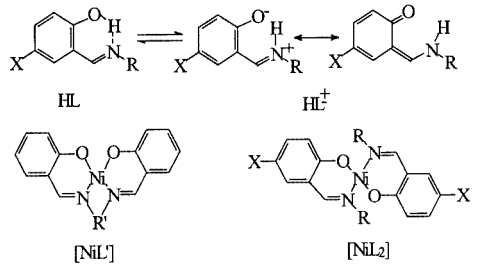

HL = 5-X-salH-R X = H; R = Et, *n*Pr; *t*Bu
X = Cl, OMe, NO_2; R = *n*Pr;
[NiL'] R' = $(CH_2)_2$, $(CH_2)_3$, 1,2-Phenyl
$[NiL_2] = [Ni(5\text{-X-sal-R})_2]$ X = H; R = Et, *n*Pr, *n*Bu
X = Cl, OMe, Me; R = *n*Pr;

Scheme 1

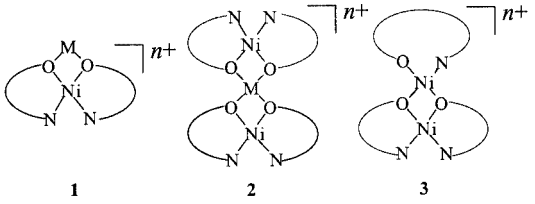

Scheme 2. Schematic representation of the interactions between tetradentate [NiL'] (N−N bridge is omitted) or bidentate $[NiL_2]$ complexes with different ions (M = alkali, alkaline earth or Ni^{II} ions; n = 1 or 2)

stricted to a few cases.[8] In solution *trans*-planar $[NiL_2]$ complexes are in equilibrium with their tetrahedral isomers when R is a bulky substituent.[9] The formation of adducts with metal ions may induce a *cis* geometry having an oxygen bite similar to that of tetradentate complexes. It has been confirmed[10,11] that 1:1 adducts are formed with Na^+ and Ba^{2+}, and 2:1 adducts with Ba^{2+} (**1** and **2** of Scheme 2) in the solid state, as well as in solution when R = H and a second pendant arm is *ortho* to the phenolato oxygen atom. From the present study it appears that $[NiL_2]$ complexes with R = alkyl group and *para* aromatic-ring substituents, may exhibit a different behaviour in the presence of Ni^{II} cations.

Results and Discussion

Reaction between HL = 5-X-salH-R and Ni^{II} Cations

The equilibrium between solvated octahedral nickel(II) and 5-X-salH-R Schiff bases for R = Et, X = H was studied in an acetonitrile solution. The spectrophotometric data were consistent with the formation of a 1:1 Ni^{II}/ligand adduct at high Ni^{II}/ligand molar ratios. A value of $\log K$ = 2.3 ± 0.01 was determined for the apparent equilibrium constant for the formation of the adduct.[12] Values of $\log K$ = 1.21 ± 0.02 and $\log K$ = 1.98 ± 0.03 were found for the formation of 1:1 adducts with Ba^{2+} and Sr^{2+}, respectively. On the basis of these findings and of the kinetic results (see below), only a 1:1 Ni^{II}/ligand product was assumed to form at the concentrations used in the kinetic measurements.

UV/Vis spectra recorded during the reaction of Ni^{II} cations with 5-X-salH-R Schiff bases (X = H, R = Et, *n*Bu; X = H, Cl, OMe, R = *n*Pr) showed different isosbestic points for the initial and final spectra, see Figure 1. At the initial reaction times a band at about 400 nm appears, while the final spectrum exhibits a maximum in the 360−370 nm range, depending on the 5-X substituent.

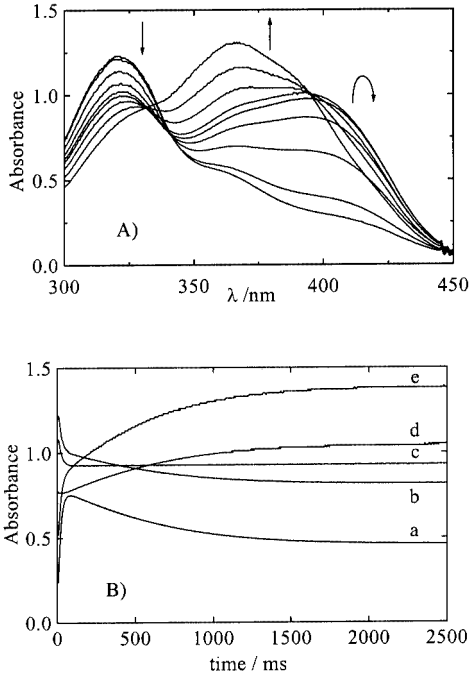

Figure 1. Spectral changes A) and kinetic traces B) at different wavelengths recorded for the reaction of 5-MeO-salH-*n*Pr (3×10^{-4} M) and nickel cations ($[Ni(CH_3CN)_6(ClO_4)_2] = 3.3 \times 10^{-2}$ M) in acetonitrile within 2500 ms at 25.0 °C (optical path = 1 cm); A) following the arrows, the spectra were recorded at 5, 10, 25, 50, 100, 250, 500, 1000, 2500 ms after mixing the reactants; B) λ = a) 416 nm, b) 332 nm, c) 322 nm, d) 394 nm, e) 366 nm

The kinetic traces could be fitted to the two-exponential Equation (10) (Exp. Sect.), which is characteristic of a two-consecutive step reaction.[13] The sum and the product of the exponential constants λ_1 and λ_2 were found to be linearly dependent on the nickel(II) concentration, Figures 2 and 3 (Figures 1*i* and 2*i*, Supporting Information). These kinetic results are in agreement with Equation (1): in the first step [Equation (1b)] the Schiff base replaces one solvent ligand leading to a mono-chelating complex; in the second step [Equation (1c)] ring closure occurs. Assuming $K_0[Ni^{2+}] << 1$, the rate constants of Equation (1) can be calculated from the slopes and the intercepts of Equations (3) and (4) (see Table 1).

$$\lambda_1 + \lambda_2 = k_f[Ni^{2+}] + (k_{-2} + k_3 + k_{-3}) \quad (3)$$

$$\lambda_1\lambda_2 = k_f(k_3 + k_{-3})[Ni^{2+}] + k_{-2}k_{-3} \quad (4)$$

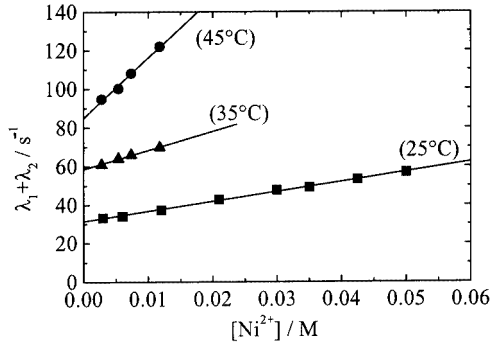

Figure 2. Plots of $\lambda_1 + \lambda_2$ [Equations (3) and (10)] against [Ni^{2+}] for the reaction between 5-H-salH-*n*Pr (ca. 10^{-4} M) and nickel(II) cations in acetonitrile at three different temperatures

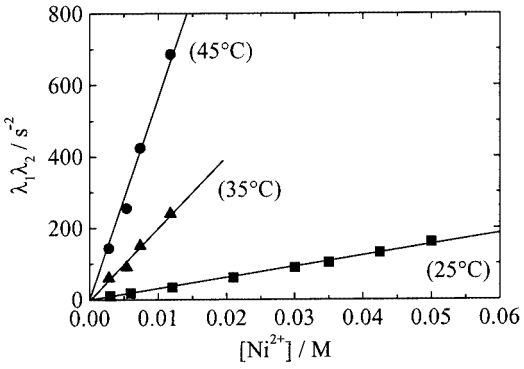

Figure 3. Plots of $\lambda_1\lambda_2$ [Equations (4) and (10)], against [Ni^{2+}] for the reaction between 5-H-salH-*n*Pr (ca. 10^{-4} M) and nickel(II) cations in acetonitrile at three different temperatures

As expected for a dissociative mechanism, the k_f rate constants were only slightly dependent on the substituent 5-X, and are close to those found for other uncharged monodentate ligands, e.g. pyridine[14] (k_f = 830 $M^{-1}s^{-1}$) and isoquinoline[15] (k_f = 709 m^{-1} s^{-1}).

The equilibrium constants K_0 for the outer-sphere complex formation were calculated from the measured k_f values as $k_f = fK_0k_{ex}$, where $k_{ex} = 3.1 \times 10^3$ s^{-1} is the rate constant of acetonitrile exchange[16] between the nickel(II) cations and the bulk solvent, and f = 3/4 is a statistical factor taking into account the number of solvent molecules in the outer-sphere complex competing with the entering ligand.[17] The theoretical K_0 values derived from the electrostatic theory, see Table 2, as well as from theoretical calculations, vide infra, were in excellent agreement.

Table 2. Calculated dipole moments of HL= 5-X-salH-R ligands, interaction energies, and theoretical and experimental equilibrium constants related to the formation of the outer-sphere complex between Ni^{II} cations and Schiff bases [Equation (1a)]

X	R	μ/Debye[a]	U[b]/kJ mol^{-1}	K_0 [c]/M^{-1}	K_0 [d]/M^{-1}
H	Et	2.44	−0.679	0.21	0.24
H	*n*Pr	2.89	−0.760	0.22	0.22
H	*t*Bu	3.63	−0.735	0.22	0.12
Cl	*n*Pr	3.31	−0.463	0.20	0.22
O_2N	*n*Pr	5.45	−0.642	0.21	0.18
MeO	*n*Pr	3.56	−0.774	0.22	0.19

[a] Dipole moment of the ligand (see text). [b] Interaction electrostatic energy between the dipole of the ligand and the charge of the nickel(II) cation. See Equation (15). [c] Theoretical K_0 values calculated by Equations (14) to (16). [d] Experimental K_0 values calculated from the ratio k_f/fk_{ex} (the values of k_f are from Table 1).

For the reaction of 5-H-salH-*n*Pr with Ni^{II} cations (Table 1), the activation parameters were $\Delta H^{\neq}$ = 34.7 ± 1.7 kJ mol^{-1} and $\Delta S^{\neq}$ = −100.4 ± 4.2 J mol^{-1} K^{-1} for k_{-2}, and $\Delta H^{\neq}$ = 71.1 ± 4.2 kJ mol^{-1}, $\Delta S^{\neq}$ = 38.5 ± 3.3 J mol^{-1} K^{-1} for k_f. The latter values compare quite satisfactorily with the activation parameters reported for solvent exchange:[17] $\Delta H^{\neq}$ = 60.8 ± 1.1 kJ mol^{-1} and $\Delta S^{\neq}$ = 25.8 J ± 2.8 J mol^{-1} K^{-1}, thus confirming a dissociative mechanism.

For X = NO_2 two well-distinct pseudo-first-order steps were confirmed. The pseudo-first-order kinetic rate constant for the first step is linearly dependent on the nickel(II) concentration, see Equation (2). For the second step, by neglecting k_{-3} and with $K_2 = k_2/k_{-2}$, Equation (5) was applied along with Equation (1). Thus the rate constants for Equation (1b) and Equation (1c) could be determined, see

Table 1. Rate constants (errors expressed as standard deviations) for the formation of 1:1 adducts between Ni^{II} cations and Schiff bases HL = 5-X-salH-R, see Equation (1)

X	R	T/°C	k_f/M^{-1} s^{-1}	k_{-2}/s^{-1}	k_3/s^{-1}	k_{-3}/s^{-1}	ΔpK_a[a]
H	Et	25.0	(5.5 ± 0.3) × 10^2 [b]	24.8 ± 0.9[b]	5.6 ± 0.4[b]	0.10 ± 0.07	
H	*n*Pr	25.0	(5.1 ± 0.1) × 10^2 [b]	25.2 ± 0.4[b]	5.6 ± 0.3[b]	0.13 ± 0.07	0.64
H	*n*Pr	35.0	(9.7 ± 0.5) × 10^2 [b]	38 ± 1[b]	20 ± 1[b]	[d]	
H	*n*Pr	45.0	(3.2 ± 0.2) × 10^3 [b]	66 ± 2[b]	18 ± 1[b]	[d]	
Cl	*n*Pr	25.0	(5.0 ± 0.2) × 10^2 [b]	40.1 ± 0.6[b]	4.4 ± 0.2[b]	[d]	0.37
O_2N	*n*Pr	25.0	(4.2 ± 0.2) × 10^2 [c]	25.2 ± 0.5[c]	0.31 ± 0.03[c]	[d]	−1.48
MeO	*n*Pr	25.0	(4.5 ± 0.1) × 10^2 [b]	33.1 ± 0.5[b]	7.5 ± 0.6[b]	0.36 ± 0.08	0.98
H	*t*Bu	25.0	(2.7 ± 0.4) × 10^2 [e]	12.5 ± 0.3[e]			
H	*t*Bu	35.0	(7.7 ± 0.6) × 10^2 [e]	19.3 ± 0.5[e]			
H	*t*Bu	45.0	(19.5 ± 0.7) × 10^2 [e]	31.8 ± 0.6[e]			

[a] $\Delta pK_a = (pK_{OH} - pK_{NH^+})$, difference between the pK_a of *p*-X-phenols[18] and *m*-X-benzylammonium[19] in water at 25 °C. [b] Calculated by Equations (10), (3) and (4). [c] Calculated according to Equations (9), (2) and (5). [d] The value of k_{-3} was neglected within the experimental error. [e] Calculated by Equations (9) and (2).

Figure 4 and Table 1, and their values confirmed the previous assumptions made on Equations (3) and (4) for the other ligands.

$$1/k_{obs(2)} = 1/(K_0K_2k_3[Ni^{2+}]) + 1/k_3 \quad (5)$$

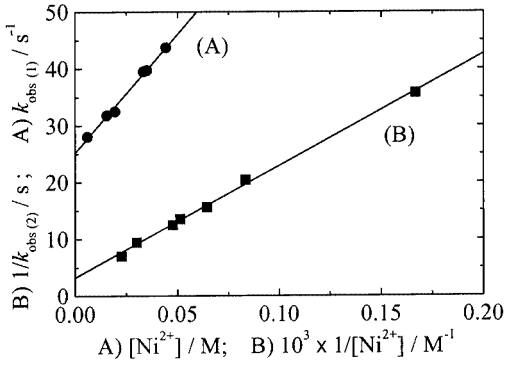

Figure 4. Plot of (A) $k_{obs(1)}$ against [Ni^{2+}] for the first reaction step [Equation (1b)] according to Equations (2) and (9), and plot of (B) $1/k_{obs(2)}$ against 1/[Ni^{2+}] for the second reaction step [Equation (1c)] according to Equations (5) and (9), for the reaction between 5-NO_2-salH-*n*Pr (ca. 10^{-4} M) and nickel(II) cations in acetonitrile at 25.0 °C

For X = H, R = *t*Bu, only one rate-determining step was seen, the final spectrum exhibits a maximum at about 390 nm. The observed pseudo-first-order rate constant depends linearly on the Ni^{II} concentration (see Figure 5) and, according to Equation (2), it could be related to the formation of the unidentate complex. The values of k_f and k_{-2} at different temperatures (Table 1) are slightly smaller than the rate constants quoted for the other ligands examined. The activation parameters, $\Delta H^{\neq}$ = 75.3 ± 1.2 kJ mol^{-1} and $\Delta S^{\neq}$ = 54.4 ± 4.2 J mol^{-1} K^{-1} for k_f and $\Delta H^{\neq}$ = 34.3 ± 2.1 kJ mol^{-1} and $\Delta S^{\neq}$ = −108.8 ± 8.4 J mol^{-1} K^{-1} for k_{-2}, are close to those found for the 5-H-salH-*n*Pr ligand. Ring closure for R = *t*Bu might be insignificant due to steric hindrance.

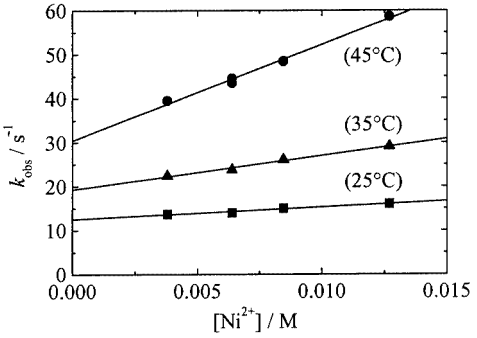

Figure 5. Plot of k_{obs} [Equations (2) and (9)] against [Ni^{2+}] for the reaction between 5-H-salH-*t*Bu (ca. 10^{-4} M) and nickel(II) cations in acetonitrile at three different temperatures

From Table 1, the rate constant k_3 for the ring-closure step depends on the substituents 5-X and increases with increasing electron-donor properties of 5-X. A linear relationship was found (slope = 0.58; correlation coefficient r = 0.999) when logk_3 is plotted vs. ΔpK_a ($\Delta pK_a = pK_{OH} - pK_{NH^+}$, where pK_{OH} [18] and pK_{NH^+} [19] are the pK_a values in water of the *p*-substituted phenols and of the *m*-substituted benzylammonium ions related to the 5-X-salH-R ligand, respectively). The positive slope suggests that migration of hydrogen from nitrogen to oxygen occurs in the ring-closure step. This agrees with a quinonic structure for the unidentate intermediate, rather than an enolic structure. The band at about 400 nm identified in the early stages of the reaction, which is characteristic[20] of the quinonic form of the ligand, confirms this proposal. Nickel(II) may be coordinated to the oxygen or the nitrogen atom of the quinonic form of the ligand, while an NH···O or N···HO intramolecular hydrogen bond is retained, respectively. Both these structures have been documented for some $MA_n \cdot mHL$ (A = anion)[4] Schiff base adducts similar to the present ones. Theoretical calculations on 5-X-salH-R ligands indicated that Ni^{II} coordination to oxygen is favoured (vide infra). A plausible mechanism for the formation of 5-X-salH-R adducts with Ni^{II} cations is depicted in Scheme 3, where solvent molecules are omitted for clarity. It is worth noting that for X = NO_2, a strong resonance stabilisation of the quinonic intermediate may account for the significantly smaller k_3 value than that observed for the other ligands.

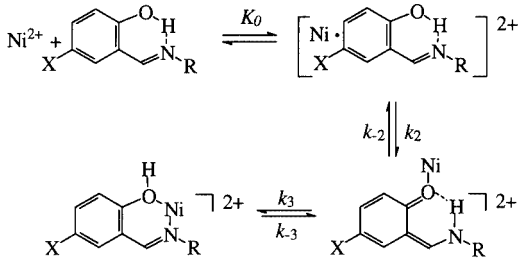

Scheme 3

Theoretical Results

The quantum-mechanical geometry optimisation shows that all the free ligands have a virtually planar geometry and that the O−H and N−H distances are 0.99 Å and 1.75−1.77 Å, respectively. These are consistent with the enolic form of HL, see Scheme 1. The computed dipole moments for the 5-X-salH-R ligands are reported in Table 2.

The most favourable arrangements for the Ni^{II}/HL outer-sphere complexes are depicted in Figure 6. In all cases the centre of the cation sphere (R = 4 Å) almost lies on the plane of the aromatic ring.

When X is an electron-donating group, the dipole moment is roughly parallel to the (HO)C−C(CH=NR) bond and the cation sphere approaches the molecule toward the oxygen atom. When X = Cl, and more so when X = NO_2, the dipole moment is rotated toward the R group and the most favourable position of the cation moves toward the aromatic ring.

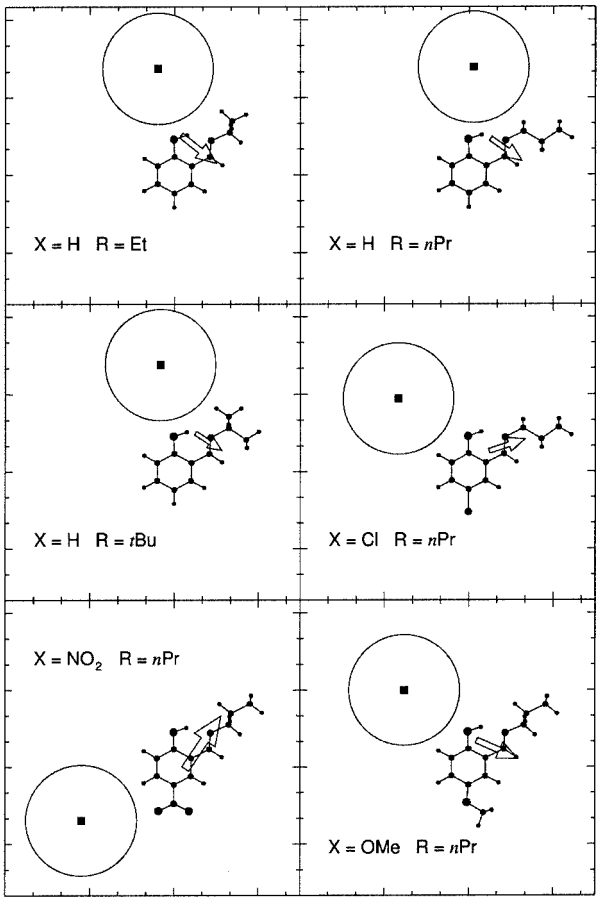

Figure 6. Schematic representation of the 5-X-salH-R/Ni^{II} outer-sphere complexes as determined by theoretical calculations; the distance between two nearest ticks of both axes is 2 Å; the molecular geometry is projected on the aromatic plane; the length of the arrow on the ligand is proportional to the dipole moment vector and indicates its position as specified in the text

When using Equations (6) and (7), a good agreement between the experimental and theoretical K_0 values (Table 2) was found. The overestimation of the theoretical K_0 value for X = H, R = *t*Bu may be of significance. The R groups are far away from the sphere of the Ni^{II} ion; nevertheless, the formation of a tighter inner-sphere complex requires the steric hindrance, that arises as a result of R, to be reduced by assuming a more favourable conformation. This cannot be achieved for R = *t*Bu.

$$K_0 = \frac{4\pi}{3000} Na^3 \times \exp(-U/k_B T) \quad (6)$$

$$U = -\frac{\mu Q \cos\alpha}{Dd^2} \quad (7)$$

In order to gain some information about the structure of the monodentate intermediate of Equation (1), we carried out a theoretical calculation on the 5-HsalH-Et ligand interaction with a cation. The effect of metal ion coordination by the ligand was studied by a simplified model system in which the NiS_5^{2+} cation was mimicked by the Na^+ cation. The cation was initially assumed to be equidistant (9 Å) from both the O and N atoms in the molecular plane of the enolic ligand. As expected, during the geometry optimisation the cation moves towards the O−H−N group, the H atom simultaneously migrates towards the N atom. The final optimised geometry (O−H = 2.09 Å, N−H = 1.03 Å) clearly shows that the presence of a cation such as Na^+ favours the quinonic form of the ligand.

Equilibria between $[NiL_2]$ = [Ni(5-X-sal-R)$_2$] Complexes and Ni^{II} Cations

The equilibria between the $[NiL_2]$ complexes and the Ni^{II} cations were studied spectrophotometrically in acetonitrile solution. On increasing the amounts of Ni^{II} cations, the characteristic MLCT and $\pi\rightarrow\pi\delta$ absorption bands[21] at ca. 400 and ca. 330 nm decrease and a new band at 370 nm appears. At high metal/ligand ratios the observed maximum shifts to longer wavelengths. (Figure 3*i*, Supporting Information). For the 5-O_2N-substituted complex, absorbance changes were too small to obtain reliable results.

Several equilibrium schemes were tested by refining the spectrophotometric data by a nonlinear least-squares program, and the formation of 1:1 or 1:2 $Ni^{II}/[NiL_2]$ adducts similar to those mentioned[2] in the introduction (see Scheme2) could be excluded. Fit residues were within the absorbance measurement error, and gave a statistical distribution at all the wavelengths examined only by applying Equation (8) (solvent molecules are omitted for clarity). In the equilibrium according to Equation (8a) the starting complex dissociates into two $[NiL]^+$ moieties. In the equilibrium according to Equation (8b) a dinuclear species $[Ni_2L_3]^+$ is formed by the interaction of $[NiL_2]$ and $[NiL]^+$.

$$[NiL_2] + Ni^{2+} \overset{K_4}{\rightleftharpoons} 2[NiL]^+ \quad (8a)$$

$$[NiL]^+ + [NiL_2] \overset{K_5}{\rightleftharpoons} [Ni_2L_3]^+ \quad (8b)$$

The related equilibrium constants, calculated as average values for at least three independent experiments, are reported in Table 3. In the present measurements, according to these values, the concentration of $[Ni_2L_3]^+$ was at most 8−10% of the total concentration of the other species.

Figure 7 shows an example of calculated spectra for the species involved in the equilibria of Equation (8) for the $Ni^{II}/[Ni(5\text{-MeO-sal-}n\text{Pr})_2]$ system; the spectrum of $[Ni_2L_3]^+$ is similar to that of $[NiL]^+$ but shows a threefold absorptivity, which is in agreement with three nearly equivalent ligands.

The ^1H NMR spectra of acetonitrile solutions of $[NiL_2]$ and Ni^{II} cations did not show detectable signals, most likely due to the presence of paramagnetic species.

A linear free energy relationship was found between the equilibrium constants $\log K_4$ of Equation (8a) and Taft's substituent constant[22] σ_p° which is related to the Schiff base oxygen atom, but not to the imine site (slope ρ° = +2.04; correlation coefficient r = 0.995) (Table 3). It is likely that an initial charge−dipole interaction between Ni^{II}

Table 3. Equilibrium constants for Equation (8) and λ_{max} [nm] of the species in solution after reaction between $[NiL_2]$ = [Ni(5-X-sal-R)$_2$] and Ni^{II} cations in acetonitrile at 25 °C

$[NiL_2]$= [Ni(5-X-sal-R)$_2$]	logK_4	logK_5	(σ°_p)[a]	$(\sigma^\circ_p - \sigma^+)$[a]	λ_{max} [b]/nm $[NiL_2]$	λ_{max} [c]/nm $[NiL^+]$	λ_{max} [c]/nm $[Ni_2L_3^+]$
[Ni(5-H-sal-Et)$_2$]	1.16 ± 0.03	3.61 ± 0.01	−	−	412	370	355
[Ni(5-H-sal-*n*Bu)$_2$]	1.03 ± 0.04	3.48 ± 0.02	−	−	413	371	360
[Ni(5-H-sal-*n*Pr)$_2$]	1.02 ± 0.03	3.50 ± 0.01	0	0	413	370	352
[Ni(5-Cl-sal-*n*Pr)$_2$]	1.64 ± 0.05	3.67 ± 0.02	0.27	0.16	420	383	355
[Ni(5-Me-sal-*n*Pr)$_2$]	0.76 ± 0.05	3.68 ± 0.02	−0.15	0.19	420	377	354
[Ni(5-MeO-sal-*n*Pr)$_2$]	0.87 ± 0.05	4.15 ± 0.01	−0.12	0.62	434	392	367

[a] Substituents constants.[22] [b] Experimental. [c] Calculated.

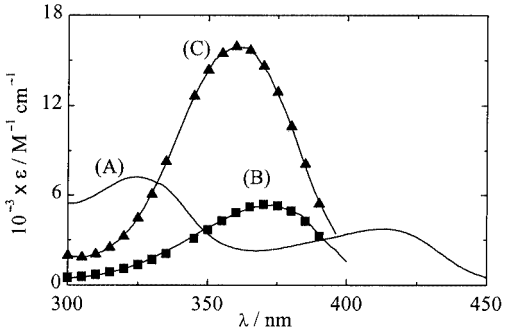

Figure 7. Experimental absorbance spectrum of $[NiL_2]$ = [Ni(5-MeO-sal-*n*Pr)$_2$] (A) and calculated absorbance spectra of $[NiL]^+$ (B), and $[Ni_2L_3]^+$ (C) in acetonitrile at 25.0 °C

cations like that in **1** in Scheme 2, yields two $[NiL]^+$ species, with electron-withdrawing substituents favouring their formation.

For logK_5, a good linear correlation was found by using the equation $\log K_5 = \rho(\sigma^\circ_p - \sigma^+)$ (slope = 0.973; r = 0.999). The interpretation of this behaviour is not straightforward since the $[Ni_2L_3]^+$ structure in solution is not known. It is likely that $[Ni_2L_3]^+$ forms by direct interaction of the starting complex $[NiL_2]$, by means of its O···O bite with the charged species $[NiL]^+$, see Scheme 2 (species **3**). This might be achieved by adopting a hindered *cis*-planar, or more likely a tetrahedral geometry. Hence, electron-withdrawing substituents on $[NiL]^+$ (which can be related to the σ^+ term) and electron-donor substituents on $[NiL_2]$ (which can be related to the σ°_p term) favour the right side of the equilibrium according to Equation (10b), accounting for the above logK_5 equation.

Experimental Section

Physical Measurements: IR and UV/Vis spectra were recorded with Perkin−Elmer 983 and Perkin−Elmer Lambda9 instruments, respectively. A Dionex Chromatograph S4000 instrument and an ICP/AES Varian Liberty 200 instrument were used for ionic chromatographic and plasma analyses, respectively. ^{1}H NMR spectra were recorded with a Varian Gemini 200 instrument.

Materials: Bis(*N*-alkyl-5-X-salicylaldiminato)nickel(II) = [Ni(5-X-sal-R)$_2$] complexes (X = H, R = Et, *n*Pr, *n*Bu; X = Cl, OMe, Me, NO_2; R = *n*Pr) were prepared and purified according to the literature.[23] *N*-Alkyl-5-X-salicylaldimine Schiff bases,[24] 5-X-salH-R (X = H; R = Et, *n*Pr, *t*Bu; X = Cl, OMe, NO_2; R = *n*Pr), were prepared by condensation of salicylaldehyde with the appropriate amine and purified by distillation under reduced pressure. Acetonitrile was purified and dried by standard methods.[25]

Caution!*: Perchlorates are potentially explosive. Only small amounts should be dried and used at once.* Alkaline earth perchlorates (Aldrich products) were dried at 100 °C under reduced pressure. Ionic HPLC and plasma analyses confirmed the purity of each salt. $[Ni(CH_3CN)_6](ClO_4)_2$ was prepared and purified according to literature methods[26] and characterised by elemental and plasma analyses.

Equilibrium and Kinetic Measurements: Spectrophotometric kinetic measurements were carried out by a stopped-flow technique previously described[27] (dead time = 6−7 ms) under dry nitrogen at different temperatures (± 0.2 °C). $[Ni(CH_3CN)_6](ClO_4)_2$ was used in a large excess (from 3×10^{-3} to 5×10^{-2} M) relative to the Schiff base ligand (ca. 10^{-4} M). The reactions were monitored by a diode-array detector (time resolution 5 ms) or a photomultiplier in the 300−500-nm UV/Vis region (time resolution 0.1 ms). Experimental kinetic traces were selected at one or more wavelengths (365, 383, 430 nm) corresponding to the largest absorbance changes. Up to six traces of absorbance (A) vs. time (t) for each kinetic run were computer-fitted to the appropriate one-exponential Equation (9), or two-exponential Equation (10). A_0 and A_∞ are the initial and final absorbances respectively, and A_1 and A_2 are pre-exponential factors. Kinetic experiments with different amounts of (nBu$_4$N)-(ClO_4) showed that the rates were not affected by ionic strength.

$$A = A_\infty + (A_0 - A_\infty) \exp(-k_{obs}t) \quad (9)$$

$$A = A_\infty + A_1 \exp(-\lambda_1 t) + A_2 \exp(-\lambda_2 t) \quad (10)$$

Equilibrium measurements were carried out as previously described.[2] 20−40 solutions of the $[NiL_2]$ complex at constant concentration (ca. 10^{-4} M) and increasing concentrations of $[Ni(CH_3CN)_6](ClO_4)_2$ were used. An inverse procedure was adopted to determine the equilibria between 5-H-salH-Et Schiff base (up to ca. 10^{-4} M) and the metal ions (ca. 10^{-3} M). The experimental absorbance $A(\lambda)$ was expressed as a function of the total concentrations C of the reactants, the absorptivities ε_λ of the species in solution and the equilibrium constants K_i according to the equilibrium scheme to be tested. Equilibrium constants and molar absorptivities at about 25 wavelengths in the range of 300 to 500 nm were simultaneously optimised using a nonlinear least-squares program.[28] Standard deviations accepted were less than 2.5×10^{-3}. Equilibria involving species at concentrations less than 2% of the total reactant were rejected.

According to Equation (8), the absorbance of an $Ni^{II}/[NiL_2]$ solution at a given wavelength λ is expressed by Equation (11), where the dependence of the ε values on the wavelength has been omitted for brevity. The mass balance equations allow to relate the concentrations of the Ni^{II} cations and $[NiL_2]$ to the total concentrations $C_{[NiL]_2}$ and $C_{[Ni^{2+}]}$.

$$A(\lambda) = \varepsilon_{Ni^{2+}}[Ni^{2+}] + \varepsilon_{NiL_2}[NiL_2] + \varepsilon_{(NiL)^+}(K_4[NiL_2][Ni^{2+}])^{1/2} + \varepsilon_{(Ni_2L_3)} + K_5[NiL_2](K_4[NiL_2][Ni^{2+}])^{1/2} \quad (11)$$

Ion pairs involving ClO_4^- anions were neglected in the acetonitrile solution.[29] In order to evaluate the activity coefficients of the charged species, the Debye−Hückel law was applied in its complete form, by taking the distance for the closest approach of the ions as $a = 5$ Å. Hence, the effect of ionic strength can be neglected for the present measurements on complexation reactions of neutral macrocyclic ligands with cations,[2] and/or for total $M(ClO_4)_2$ concentrations not exceeding 0.001 M.

Computational Details: The geometry of the 5-X-salH-R ligands was optimised by employing the Density Functional Theory based on the B3LYP functional.[30]The triple zeta with polarisation 6−311G* basis set was employed and the calculations were carried out with the Gaussian98[31] package. Other calculations concerning some species involved in the reaction of Ni^{II} cations with HL ligands were performed in the same way.

With the aim to evaluate the $[NiS_6]^{2+}$/HL (S = solvent) interaction energy of the outer-sphere complex, we resorted to the Fuoss association theory[32,33] (originally developed for ions in a solvent), represented as a polarizable continuum and adapted to the case of an ion interacting with a dipole. If the cation is considered as a point charge at the centre of a sphere of radius a, then the equilibrium constant K_0 can be approximated as in Equation (6), where a is expressed in cm, N is the Avogadro number, and U is the charge−dipole electrostatic interaction energy. By considering the solvent as a continuum of permittivity D, the energy U may be approximated to the lowest power of the charge−dipole distance d as in Equation (7), where μ is the dipole moment and α is the angle between the dipole vector and the electric field generated by the charge Q at the dipole centre. Unfortunately, this simple theoretical approach, in which the ligand dipole is placed at a fixed distance from the positive sphere and is directed towards the more favourable direction, cannot properly account for the geometrical factors of the ligands. Thus, we use a more sophisticated approach, in which each atom both of the $[NiS_6]^{2+}$ and of the ligand has been represented as a hard sphere with the appropriate van der Waals radius. The energy was calculated again using Equation (7), by placing the ligand dipole in the middle of the segment connecting the centre of the charge originated by the positively charged atoms of the ligand, to the centre of the charge arising from the negatively charged atoms [Equation (12)], where c is the centre of the dipole and k runs over the positively charged ligand atoms.

$$\vec{c} = 2\left(\sum_j^{pos} q_j\right)^{-1} \sum_k^{all} q_k \vec{R}_k \quad (12)$$

The atomic charges q were determined by the Mulliken population analysis method. The most favourable conformations were determined by starting from a large number of geometrical arrangements of the cation−ligand system and moving the molecules along the energy gradient until an energy minimum was found.

Supporting Information: See footnote on the first page of this article. Plots of $\lambda_1 + \lambda_2$ and of $\lambda_1\lambda_2$ against $[Ni^{2+}]$ for the reaction between 5-X-salH-R (ca. 10^{-4} M) and nickel(II) cations in acetonitrile at 25.0 °C; 5-X-salH-R = 5-Cl-salH-*n*Pr; 5-H-salH-Et; 5-MeO-salH-*n*Pr. UV/Vis spectra of $[Ni(5\text{-H-sal-Et})_2]$ in the presence of different amounts of $Ni(CH_3CN)_6(ClO_4)_2$ in an acetonitrile solution.

Acknowledgments

These studies were supported by the Consiglio Nazionale delle Ricerche (CNR, Roma) and by the Ministero dell'Università e della Ricerca Scientifica e Tecnologica, Ricerche di Rilevante Interesse Nazionale 2000−1. We thank Prof. F. Calderazzo for helpful discussions.

[1] A. Mederos, S. Dominguez, R. Hernandez-Molina, J. Sanchiz, F. Brito, *Coord. Chem. Rev.* **1999**, *193−195*, 857.
[2] L. Carbonaro, M. Isola, P. La Pegna, L. Senatore, *Inorg. Chem.* **1999**, *38*, 5519, and references therein.
[3] J. G. Muller, L. A. Kayser, S. J. Paikoff, V. Duarte, N. Tang, R. J. Perez, S. E. Rokita, C. J. Burrows, *Coord. Chem. Rev.* **1999**, *185−186*, 761.
[4] A. D. Garnovskii, A. L. Nivorozhkin, V. I. Minkin, *Coord. Chem. Rev.* **1993**, *126*, 1.
[5] [5a] J. Burgess in *Metal Ions in Solution*, Ellis Horwood, Chichester, **1978**, chapters 11 and 12. [5b]C. P. Kulatilleke, S. N. Goldie, M. J. Heeg, L. A. Ochrymowyez, D. B. Rorabacher, *Inorg. Chem.* **2000**, *39*, 1444, and references therein.
[6] C. M. Metzler, A. Cahill, D. Metzler, *J. Am. Chem. Soc.* **1980**, *102*, 6075.
[7] Z. Rozwadowski, E. Majewski, T. Dziembowska, P. E. Hansen, *J. Chem. Soc., Perkin Trans. 2* **1999**, 2809.
[8] [8a] R. J. Butcher, J. Jasinski, G. M. Mockler, E. Sinn, *J. Chem. Soc., Dalton Trans.* **1976**, 1099. [8b] O. F. Shall, K. Robinson, J. L. Atwood, G. W. Gokel, *J. Am. Chem. Soc.* **1991**, *113*, 7434. [8c] O. F. Shall, K. Robinson, J. L. Atwood, G. W. Gokel, *J. Am. Chem. Soc.* **1993**, *115*, 5962.
[9] R. H. Holm, M. J. O'Connor in *Progress in Inorganic Chemistry*, Wiley-Interscience, New York, **1971**, vol. 14, p. 241.
[10] J. P. Costes, F. Dahan, J. P. Laurent, *Inorg. Chem.* **1994**, *33*, 2738.
[11] J. P. Costes, J. P. Laurent, P. Chabert, G. Commenges, F. Dahan, *Inorg. Chem.* **1997**, *36*, 656, and references cited therein.
[12] The apparent equilibrium constant K is defined as $K = K_0K_2 + K_0K_2K_3$ in the case that Equation (1) applies to the reaction. For Ni^{II}/5-H-salH-Et, by introducing the kinetic rate constants k_2, k_{-2}, k_3 (see below), a calculated value of $k_{-3} = 0.73 \pm 0.63$ s^{-1} can be compared with the value of 0.10 ± 0.07 s^{-1} determined kinetically, see text.
[13] R. G. Wilkins, in *Kinetics and Mechanism of Reactions of Transition Metal Complexes*, 2nd ed., VCH, Weinheim, **1991**.
[14] P. K. Chattopadhyay, J. F. Coetzee, *Inorg. Chem.* **1973**, *12*, 113.
[15] The rate constant is reported in the molal scale as originally expressed by: K. Ishihara, S. Funahashi, M. Tanaka, *Inorg. Chem.* **1983**, *22*, 2567.
[16] Y. Yano, M. T. Fairhurst, T. W. Swaddle, *Inorg. Chem.* **1980**, *19*, 3267.
[17] J. Neely, R. Connick, *J. Am. Chem. Soc.* **1970**, *92*, 3476.
[18] A. Brändström, *J. Chem. Soc., Perkin Trans. 2* **1999**, 1847, and references therein.
[19] L. F. Blackwell, A. Fischer, I. J. Miller, R. D. Topsom, J. Vaugham, *J. Chem. Soc.* **1964**, 3588.
[20] K. K. Chatterjee, B. E. Douglas, *Spectrochim. Acta* **1964**, 1625.
[21] S. Di Bella, I. Fragalà, I. Ledoux, M. Diaz-Garcia, T. J. Marks, *J. Am. Chem. Soc.* **1997**, *119*, 9550.
[22] R. W. Taft, Jr., *J. Phys. Chem.* **1960**, *64*, 1805.
[23] [23a] L. Sacconi, M. Ciampolini, N. Nardi, *J. Am. Chem. Soc.*

1964, *86*, 819; E. Frasson, C. Panattoni, L. Sacconi, *J. Phys. Chem.* **1959**, *63*, 1908. [23b] R. H. Holm, *J. Am. Chem. Soc.* **1961**, *83*, 4683.
[24] H. Schiff, *Ann. Chem. Pharm.* **1869**, *150*, 193.
[25] J. F. Coetzee, *Progress in Physical Organic Chemistry*, Interscience, New York, **1967**, vol. 4.
[26] A. E. Wickenden, R. A. Krause, *Inorg. Chem.* **1965**, *4*, 404.
[27] L. Carbonaro, L. Guogang, M. Isola, L. Senatore, *Inorg. Chim. Acta* **2000**, *303*, 40.
[28] R. Ambrosetti, D. Ricci, R. Bianchini, *Gazz. Chim. Ital.* **1997**, *127*, 567.
[29] W. Libus, H. Strzelecki, *Electrochim. Acta* **1970**, *15*, 703.
[30] A. D. Becke, *J. Chem. Phys.* **1993**, *98*, 5648.
[31] M. J. Frisch, G. W. Trucks, H. B. Schlegel, G. E. Scuseria, M. A. Robb, J. R. Cheeseman, V. G. Zakrzewski, J. A. Montgomery, R. E. Stratmann, J. C. Burant, S. Dapprich, J. M. Millam, A. D. Daniels, K. N. Kudin, M. C. Strain, O. Farkas, J. Tomasi, V. Barone, M. Cossi, R. Cammi, B. Mennucci, C. Pomelli, C. Adamo, S. Clifford, J. Ochterski, G. A. Petersson, P. Y. Ayala, Q. Cui, K. Morokuma, D. K. Malick, A. D. Rabuck, K. Raghavachari, J. B. Foresman, J. Cioslowski, J. V. Ortiz, B. B. Stefanov, G. Liu, A. Liashenko, P. Piskorz, I. Komaromi, R. Gomperts, R. L. Martin, D. J. Fox, T. Keith, M. A. Al-Laham, C. Y. Peng, A. Nanayakkara, C. Gonzalez, M. Challacombe, P. M. W. Gill, B. G. Johnson, W. Chen, M. W. Wong, J. L. Andres, M. Head-Gordon, E. S. Replogle, J. A. Pople, *Gaussian 98* (Revision A.7), Gaussian, Inc., Pittsburgh, PA, **1998**.
[32] R. M. Fuoss, *J. Am. Chem. Soc.* **1958**, *80*, 5059.
[33] J. Williams, S. Petrucci, B. Sesta, M. Battistini, *Inorg. Chem.* **1974**, *13*, 1968.

Received November 23, 2001
[I01475]